Multicarrier transport in epitaxial multilayer graphene

Yu-Ming Lin,[1,a)] Christos Dimitrakopoulos,[1] Damon B. Farmer,[1] Shu-Jen Han,[1] Yanqing Wu,[1] Wenjuan Zhu,[1] D. Kurt Gaskill,[2] Joseph L. Tedesco,[2] Rachael L. Myers-Ward,[2] Charles R. Eddy, Jr.,[2] Alfred Grill,[1] and Phaedon Avouris[1]
[1]*IBM T.J. Watson Research Center, Yorktown Heights, New York 10598, USA*
[2]*Advanced SiC Epitaxial Research Laboratory, U.S. Naval Research Laboratory, Washington DC 20375, USA*

(Received 9 July 2010; accepted 12 August 2010; published online 15 September 2010)

Variable-field Hall measurements were performed on epitaxial graphene grown on Si-face and C-face SiC. The carrier transport involves essentially a single-type of carrier in few-layer graphene, regardless of SiC face. However, in multilayer graphene (MLG) grown on C-face SiC, the Hall measurements indicated the existence of several groups of carriers with distinct mobilities. Electrical transport in MLG can be properly described by invoking three independent conduction channels in parallel. Two of these are n- and p-type, while the third involves nearly intrinsic graphene. The carriers in this lightly doped channel have significantly higher mobilities than the other two. © *2010 American Institute of Physics*. [doi:10.1063/1.3485671]

Significant attention has been focused recently on the electrical properties of graphene grown epitaxially on SiC substrates,[1,2] because it offers an ideal platform for carbon-based electronics. Recent advances in graphene growth and device fabrication have led to demonstrations of field-effect transistors made from epitaxial graphene with radio-frequency performance exceeding that of their Si-based counterparts.[3,4]

The layer structure and electrical properties of graphene films grown on Si-terminated versus C-terminated surfaces of the SiC substrate are quite different.[2] Graphene growth is much faster on the C-face, so that at the same growth temperature, multiple layers of graphene are more readily formed on the C-face than on the Si-face substrates. Nevertheless, the conductive carbon films produced on either crystal face of SiC possess the honeycomb lattice structure and the transport characteristics unique to graphene.[5] There is also mounting evidence that multilayer graphene (MLG) films grown on the C-face SiC are typically rotationally disordered with a band structure similar to that of an individual graphene monolayer.[6]

Hall measurements performed at a single magnetic field yield a weighted average of carrier mobility and density, and are strictly applicable to homogeneous samples. In this respect, *single-layer graphene* is ideal since it is a truly two-dimensional material with a single conduction (or valence) band at any Fermi energy. As a result, the carrier density and mobility in single-layer graphene have been accurately determined by Hall measurements based on a single-carrier model. However, results obtained from such measurements are not likely to be representative of transport properties in MLG, where carriers may possess different mobilities in different graphene layers. In the C-face MLG, cyclotron resonance measurements typically yield much higher carrier mobilities than those obtained from direct electrical measurements,[7,8] suggesting nonhomogeneous carriers in the system. In this study, we performed variable-field Hall and resistivity measurements on epitaxial graphene, and the results were analyzed with a multicarrier model. Good agreements were obtained between experimental data and the model, providing evidence of multicarrier transport in the C-face grown MLG.

Epitaxial graphene films studied here were synthesized on semi-insulating 4H–SiC (Cree) and 6H–SiC (II-VI, Inc.) substrates. To avoid factors specific to the reactor and/or growth conditions, we investigated graphene samples produced from two laboratories, IBM and NRL. The details of the two synthesis protocols are reported elsewhere.[9,10] Metal contacts made of Pd/Au were patterned using either e-beam or optical lithography. The Hall bar geometry of the graphene channel was then defined by oxygen plasma etching using PMMA as the etch mask. Inset of Fig. 1(b) shows the scanning electron microscope (SEM) image of a six-contact graphene Hall bar device fabricated on C-face SiC with a width of 4 μm and length of 30 μm between the voltage probes. Variable-field resistivity and Hall measurements were performed between 0 and 1 Tesla and carried out in high vacuum ($\sim 10^{-8}$ torr) at room temperature.

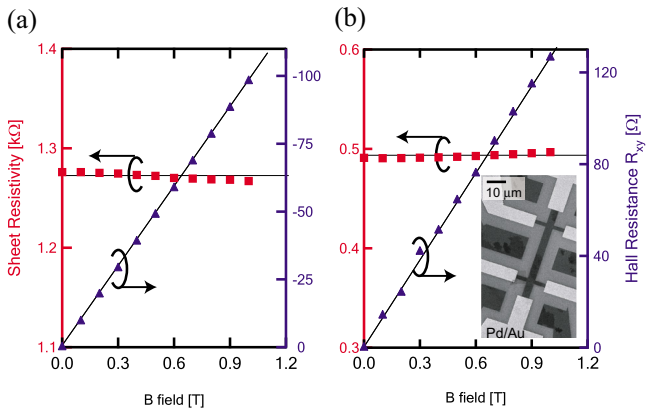

FIG. 1. (Color online) Measured sheet resistivity ρ_{xx} and Hall resistance R_H as a function of magnetic field for thin graphene layers grown on (a) Si-face SiC and (b) C-face SiC. Both graphene samples were synthesized at IBM. The solid lines represent expected field dependence in a single-carrier model. Inset: SEM image of a Hall bar device fabricated on C-face epitaxial graphene.

a)Electronic mail: yming@us.ibm.com.

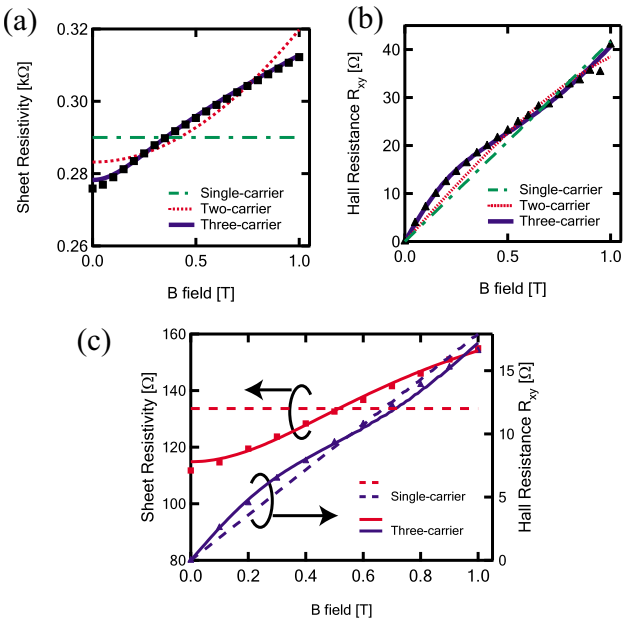

FIG. 2. (Color online) Measured (a) sheet resistivity ρ_{xx} and (b) Hall resistance R_H as a function of magnetic field for multilayer graphene grown on C-face SiC. The experimental data are represented by the symbols. The dashed-dotted, dashed, and solid curves result from least-squares fitting of the data using the single-, two-, and three-carrier model, respectively. (c) Measured ρ_{xx} and R_H of another MLG Hall bar device fabricated on a different C-face SiC substrate. The graphene sample shown in (a) and (b) was produced at IBM while the sample shown in (c) was produced at NRL.

Figures 1(a) and 1(b) show the measured sheet resistivity ρ_{xx} and Hall resistance R_H as a function of magnetic field for thin graphene layers grown from Si-face and C-face SiC substrates, respectively. The number of graphene layers in these devices, determined by Raman spectroscopy and optical adsorption of the SiC peak,[11] is 1–2 layers on the Si-face and two to four layers on the C-face SiC substrates. In both type of devices, ρ_{xx} remains nearly constant (within 0.5%) and R_H, is linearly proportional to the magnetic field, exhibiting excellent agreement with the transport behavior involving only a single type of carrier. In a single-carrier system, ρ_{xx} and R_H, are determined by the carrier density, n_H, and Hall mobility, μ_H, through the relations $R_H = B \cdot (qn_H)^{-1}$ and $\rho_{xx} = (qn_H\mu_H)^{-1}$, where q is the electron charge. Thus, from Figs. 1(b) and 1(c), the carrier density and mobility can be unambiguously determined, yielding for the specific samples $n_H = 6.3 \times 10^{12}$ cm^{-2} (n-type) and $\mu_H = 800$ cm^2/V s for graphene grown on Si-face SiC, and $n_H = 4.9 \times 10^{12}$ cm^{-2} (p-type) and $\mu_H = 2590$ cm^2/V s for C-face sample. Multiple devices have been measured on the same C-face and Si-face substrates, and they all exhibit field-dependent transport behavior well described by the single-carrier model.

For thicker graphene layers, the results from Hall measurements exhibit drastically different behaviors. Figures 2(a) and 2(b) show the measured ρ_{xx} and R_H of a Hall bar device fabricated on MLG grown on C-face SiC at IBM. The number of graphene layers on this substrate is estimated to be more than ten. In Figs. 2(a) and 2(b), $\rho_{xx}(B)$ increases with increasing field, varying by more than 15% at $B = 1$ T, and $R_H(B)$ exhibits a nonlinear field dependence. The best fitted results using the single-carrier model are shown by the dashed-dotted curves in Figs. 2(a) and 2(b), exposing significant deviation from the measured data. This deviation prohibits the unique determination of the carrier density and mobility from Hall measurements performed at a single B-field. The nonlinear field dependence of R_H indicates the existence of carriers with different mobilities,[12] and possibly different polarities in MLG.

In an electronic system with N types of distinct mobility carriers, the conductivity tensor $\boldsymbol{\sigma}$ (the inverse of the resistivity tensor) in a magnetic field applied perpendicular to the transport plane is given by the following:

$$\sigma_{xx}(B) = \sum_i^N \frac{n_i q \mu_i}{1 + \mu_i^2 B^2}, \quad \sigma_{xy}(B) = \sum_i^N \frac{n_i q \mu_i^2 B}{1 + \mu_i^2 B^2}. \tag{1}$$

For a given N, a least-square fit of Eq. (1) can then be performed on the measured data at various magnetic fields to yield the mobility and density of each carrier type. While an *a priori* assumption on N is required, in practice, one usually starts with a small test value of N and incrementally increases it until the fit converges to the measured data. For $N=2$, the multicarrier analysis yields mobilities of $\mu_1 = 5800$ and $\mu_2 = 1650$ cm^2/V s with corresponding carrier densities of $n_1 = 1.7 \times 10^{12}$ (hole) and $n_2 = 7.4 \times 10^{12}$ cm^{-2} (electron). Despite some improvements, there remains significant discrepancy in terms of the absolute error and the trend in field dependence [see dashed curves in Figs. 2(a) and 2(b)], indicating the deficiency of the two-carrier assumption for this sample. Excellent agreement between the measurements and simulation is achieved with $N=3$, as shown by the solid curves in Figs. 2(a) and 2(b). The three-carrier model yields carrier mobilities of $\mu_1 = 1840$, $\mu_2 = 28500$, and $\mu_3 = 6900$ cm^2/V s, with the corresponding carrier densities of $n_1 = 9.9 \times 10^{12}$ (hole), $n_2 = 5.3 \times 10^{10}$ (hole), and $n_3 = 3.7 \times 10^{11}$ cm^{-2} (electron). While there is no fundamental limit on N in the modeling of MLG, the three-carrier model is able to provide good agreement with experimental results (both ρ_{xx} and R_H) from all the C-face MLG samples synthesized at our two laboratories. Another example in Fig. 2(c) shows the Hall measurements of MLG (~50 layers) grown on a different C-face SiC substrate. A similar discrepancy from the single-carrier behavior (shown by dashed curves) is observed, whereas the three-carrier transport model (solid curves) captures all the essential features of the field dependence in the measured data. The extracted carrier mobilities are $\mu_1 = 1500$, $\mu_2 = 19300$, and $\mu_3 = 12400$ cm^2/V s with corresponding carrier densities of $n_1 = 2.3 \times 10^{13}$ (hole), $n_2 = 5.1 \times 10^{11}$ (hole), and $n_3 = 7.7 \times 10^{11}$ cm^{-2} (electron). For comparison, the single-carrier model yields a hole carrier density of 3.5×10^{13} cm^{-2} and a mobility of 1340 cm^2/V s, which clearly does not reflect the carriers present.

The method of multicarrier analysis has been previously employed to characterize transport properties in heterostructures such as Al-GaAs, InP/InAlGaAs, and bulk InN.[12] In bulk materials, the multicarrier transport could arise from the presence of multiple carrier pockets in the Brillouin zone, while in a multilayered structure this could result from carriers with different mobilities residing at separate layers. In MLG grown on the C-face SiC, the multicarrier transport is not likely to be attributed to the former, because the simple, conical band structure is largely preserved. Instead, the distinct carrier mobilities suggest transport involving independent carriers in different layers of the MLG. Although the band structure of the rotationally disordered MLG system is similar to that of an individual monolayer, there is still small

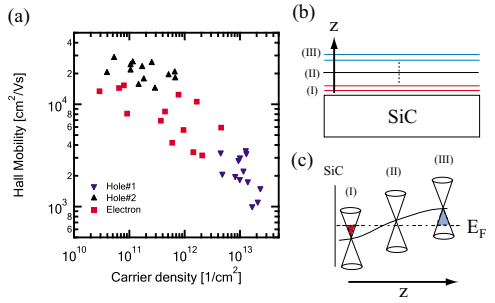

FIG. 3. (Color online) (a) Hall mobility as a function of carrier density, extracted using the three-carrier analysis, for 13 graphene devices fabricated from five different C-face SiC substrates with more than ten graphene layers. (b) Schematics of multilayer graphene grown on C-face SiC, showing the three dominant channels involving layers with different doping and transport properties. (c) Schematics of the doping profile of epitaxial graphene multilayers.

coupling between the layers,[13] which would allow electrical conduction between them. Previous studies have shown that the first few graphene layers close to the SiC substrate are heavily doped, with the doping level decreasing away from the interface.[14,15] Since the carrier mobility of graphene depends on the carrier density[16] and is also sensitive to sources of scattering in the environment, it is expected that graphene layers at different distances from the substrates would possess different mobilities.

Using the multicarrier analysis, Fig. 3(a) shows the measured Hall mobility as a function of carrier density for 13 graphene devices fabricated from five different C-face SiC substrates with more than ten graphene layers. All devices exhibit magneto-transport behaviors similar to those shown in Fig. 2, where good agreement with the data is obtained using the three-carrier model. Fig. 3(a) suggests that electrical transport in the measured C-face MLG is dominated by three groups of carriers: one involves a higher density of holes with mobilities below 4000 $cm^2/V\,s$, one with a lower density of holes with high mobilities in excess of 10000 $cm^2/V\,s$, and one with electrons with mobilities above 3000 $cm^2/V\,s$. We note that while the multicarrier analysis does not reflect the exact number of graphene layers in the sample participating in transport, the electrical transport of the entire graphene stack can be effectively described by only three conduction channels with different average mobilities and densities. Since epitaxial MGL are heavily n-type in the vicinity of the SiC interface[1,14] and become nearly intrinsic in subsequent layers,[15] we attribute the *n*-type channel (I) to the first few graphene layers near the SiC substrate, the lightly *p*-type channel (II) to the subsequent layers, and the heavily p-type channel (III) to the uppermost layers, as shown in Fig. 3(b). The doping profile of epitaxial MLG is schematically shown in Fig. 3(c). In the lightly-doped channel (II), carriers are effectively screened from the charged scattering sources by the underlying and overlaying graphene layers, allowing for the highest carrier mobility among the three conduction channels. While high carrier mobilities in the quasi-intrinsic part of the MLG have also been previously investigated by far infrared optical absorption techniques,[7,8] the results and analysis shown here present the evidence of such high mobility carriers in electrical measurements.

In summary, we show that transport in thin epitaxial graphene is essentially a single-carrier type regardless of the SiC face. In thick MLG grown on C-face SiC, however, electrical transport involves multiple types of carriers with different mobilities in different graphene layers. High mobilities are preserved in the quasi-intrinsic graphene region sandwiched between the underlying and overlaying conducting layers.

The authors would like to thank V. Perebeinos, C. Y. Sung, Y. Sun, and F. Xia for insightful discussions, M. Freitag for Raman characterization, and B. Ek and J. Bucchignano for the expert technical assistance. J. L. Tedesco is grateful for postdoctoral support from ASEE. This work is supported by DARPA under Contract No. FA8650-08-C-7838 through the CERA program and by the Office of Naval Research.

[1] C. Berger, Z. Song, T. Li, X. Li, A. Y. Ogbazghi, R. Feng, Z. Dai, A. N. Marchenkov, E. H. Conrad, P. N. First, and W. A. de Heer, J. Phys. Chem. B **108**, 19912 (2004).
[2] P. N. First, W. A. de Heer, T. Seyller, C. Berger, J. A. Stroscio, and J.-S. Moon, MRS Bull. **35**, 296 (2010).
[3] Y.-M. Lin, C. Dimitrakopoulos, K. A. Jenkins, D. B. Farmer, H.-Y. Chiu, A. Grill, and P. Avouris, Science **327**, 662 (2010).
[4] J. S. Moon, D. Curtis, S. Bui, M. Hu, D. K. Gaskill, J. L. Tedesco, P. Asbeck, G. G. Jernigan, B. L. VanMil, R. L. Myers-Ward, C. R. Eddy, Jr., and P. M. Campbell, IEEE Electron Device Lett. **31**, 260 (2010).
[5] T. Shen, J. J. Gu, M. Xu, Y. Q. Wu, M. L. Bolen, M. A. Capano, L. W. Engel, and P. D. Ye, Appl. Phys. Lett. **95**, 172105 (2009).
[6] X. Wu, X. Li, Z. Song, C. Berger, and W. A. de Heer, Phys. Rev. Lett. **98**, 136801 (2007).
[7] M. Orlita, C. Faugeras, P. Plochocka, P. Neugebauer, G. Martinez, D. K. Maude, A.-L. Barra, M. Sprinkle, C. Berger, W. A. de Heer, and M. Potemski, Phys. Rev. Lett. **101**, 267601 (2008).
[8] G. G. Jernigan, B. L. VanMil, J. L. Tedesco, J. G. Tischler, E. R. Glaser, A. Davidson III, P. M. Campbell, and D. K. Gaskill, Nano Lett. **9**, 2605 (2009).
[9] C. Dimitrakopoulos, Y.-M. Lin, A. Grill, D. B. Farmer, M. Freitag, Y. Sun, S.-J. Han, Z. Chen, K. A. Jenkins, Y. Zhu, Z. Liu, T. J. McArdle, J. A. Ott, R. Wisnieff, and P. Avouris, J. Vac. Sci. Technol. B **28**, 985 (2010).
[10] J. L. Tedesco, B. VanMil, R. L. Myers-Ward, J. Culbertson, G. Jernigan, P. Campbell, J. M. McCrate, S. A. Kitt, C. Eddy, Jr., and D. K. Gaskill, ECS Trans. **19**(5), 137 (2009).
[11] S. Shivaraman, M. V. S. Chandrashekhar, J. J. Boeckl, and M. G. Spencer, J. Electron. Mater. **38**, 725 (2009).
[12] N. Biyikli, J. Xie, Y.-T. Moon, F. Yun, C.-G. Stefanita, S. Bandyopadhyay, H. Morkoç, I. Vurgaftman, and J. R. Meyer, Appl. Phys. Lett. **88**, 142106 (2006).
[13] E. J. Mele, Phys. Rev. B **81**, 161405(R) (2010).
[14] D. Sun, C. Divin, C. Berger, W. A. de Heer, P. N. First, and T. B. Norris, Phys. Rev. Lett. **104**, 136802 (2010).
[15] M. L. Sadowski, G. Martinez, and M. Potemski, Phys. Rev. Lett. **97**, 266405 (2006).
[16] W. Zhu, V. Perebeinos, M. Freitag, and P. Avouris, Phys. Rev. B **80**, 235402 (2009).